NASA/TM—2000-209270

# A Note on Trapping Moving Vortices

Hsiao C. Kao
Glenn Research Center, Cleveland, Ohio

July 2000

## The NASA STI Program Office . . . in Profile

Since its founding, NASA has been dedicated to the advancement of aeronautics and space science. The NASA Scientific and Technical Information (STI) Program Office plays a key part in helping NASA maintain this important role.

The NASA STI Program Office is operated by Langley Research Center, the Lead Center for NASA's scientific and technical information. The NASA STI Program Office provides access to the NASA STI Database, the largest collection of aeronautical and space science STI in the world. The Program Office is also NASA's institutional mechanism for disseminating the results of its research and development activities. These results are published by NASA in the NASA STI Report Series, which includes the following report types:

- TECHNICAL PUBLICATION. Reports of completed research or a major significant phase of research that present the results of NASA programs and include extensive data or theoretical analysis. Includes compilations of significant scientific and technical data and information deemed to be of continuing reference value. NASA's counterpart of peer-reviewed formal professional papers but has less stringent limitations on manuscript length and extent of graphic presentations.

- TECHNICAL MEMORANDUM. Scientific and technical findings that are preliminary or of specialized interest, e.g., quick release reports, working papers, and bibliographies that contain minimal annotation. Does not contain extensive analysis.

- CONTRACTOR REPORT. Scientific and technical findings by NASA-sponsored contractors and grantees.

- CONFERENCE PUBLICATION. Collected papers from scientific and technical conferences, symposia, seminars, or other meetings sponsored or cosponsored by NASA.

- SPECIAL PUBLICATION. Scientific, technical, or historical information from NASA programs, projects, and missions, often concerned with subjects having substantial public interest.

- TECHNICAL TRANSLATION. English-language translations of foreign scientific and technical material pertinent to NASA's mission.

Specialized services that complement the STI Program Office's diverse offerings include creating custom thesauri, building customized data bases, organizing and publishing research results . . . even providing videos.

For more information about the NASA STI Program Office, see the following:

- Access the NASA STI Program Home Page at ***http://www.sti.nasa.gov***

- E-mail your question via the Internet to help@sti.nasa.gov

- Fax your question to the NASA Access Help Desk at (301) 621-0134

- Telephone the NASA Access Help Desk at (301) 621-0390

- Write to:
  NASA Access Help Desk
  NASA Center for AeroSpace Information
  7121 Standard Drive
  Hanover, MD 21076

NASA/TM—2000-209270

# A Note on Trapping Moving Vortices

Hsiao C. Kao
Glenn Research Center, Cleveland, Ohio

National Aeronautics and
Space Administration

Glenn Research Center

July 2000

This report contains preliminary findings, subject to revision as analysis proceeds.

Available from

NASA Center for Aerospace Information
7121 Standard Drive
Hanover, MD 21076
Price Code: A03

National Technical Information Service
5285 Port Royal Road
Springfield, VA 22100
Price Code: A03

# A Note on Trapping Moving Vortices

Hsiao C. Kao
National Aeronautics and Space Administration
Glenn Research Center
Cleveland, Ohio 44135

## Summary

The topic of stationary configurations of point vortices, also known as vortex equilibrium, has received considerable attention in recent years. By observing numerical results, it is found that a "counterpart" of this system also exists, in which moving vortices may be "trapped" by an inlet-like device to form a stationary pattern with no translational motion. After an intuitive explanation for the process, vortex trajectory maps based on numerical results are presented. These maps exhibit two stationary points under the present conditions, which are the focal points of vortex trajectories. A vortex upstream of these points, if within a certain offset range, will move towards these points spontaneously and be captured there. This proposed device is also capable of trapping spinning vortex pairs and triads. It is possible to impose a uniform stream at infinity, as long as the flow field is still dominated by the moving vortices.

## 1. Introduction

In view of the fact that vortices are considered to be the "sinews and muscles" of fluid dynamics and often used for aerodynamic performance improvements, the study of vortex dynamics has received enduring attention. New applications and properties have been uncovered. In a review paper by Aref, Kadtke, Zawadzki, Campbell and Eckhart (1988), the authors discussed the topic of vortex equilibrium, in which n point vortices of strength +1 and m point vortices of strength −1 form a completely stationary system with no translational motion.

Numerical results obtained in this study suggest that a "counterpart" of this system also exists, in which moving vortices may be "trapped" by an inlet-like device to form a stationary configuration with no translational motion. In order to illustrate this situation, we go to figure 1. In this figure, a pair of spinning vortices moving from left to right in a body of otherwise still fluid is being trapped by the device. The dashed line at the bottom is the ground surface. Thus, there is an image system below the surface. If no device is present, this pair of free spinning vortices translates parallel to the surface at a constant speed. When a device is introduced, an interaction takes place. In this case, the free vortices establishes the flow field and the combined effect of the vortices and the device determines the vortex paths. This assumption of no free stream velocity may be removed as long as the dominant flow field is still due to free vortices. A brief discussion and some numerical results will be given later. This situation is somewhat similar to Foppl's standing vortex pair behind a circular cylinder (Saffman, 1992).

The vortex pair in figure 1 is of the same strength and same sense, spins about its centroid and moves downstream at the same time. If its initial position is within a certain offset distance from the device centerline, it is liable to be trapped. A heavy black circle in the plot is a testimony of this state, in which two vortices rotate about an essentially stationary centroid. The pattern in figure 1 represents the vortex trajectory paths after 9800 time steps. Although it needed only 3200 time steps to reach the stationary zone, the extra 6600 steps were added to demonstrate the immobility of the centroid. Here we use a spinning pair to bring out a more dynamic picture, even though a single vortex is the main topic of this note.

We now give an intuitive explanation of this process with a single moving vortex. To do this, we refer to the surface vorticity method for the potential flow by Martensen (1959). In addition to this original work, there are many papers dealing with this method but we cite only Lewis (1981 and 1991). For calculating the potential flow around one or more arbitrary bodies, this method places a continuous distribution of vorticity elements on the body surfaces to separate the outer flow from the inner region of zero velocity. In the present case of zero free stream velocity, the potential flow is due solely to the moving vortices. Thus, the strengths of these surface vorticity elements have to adjust continuously to satisfy the surface condition and are functions of time. Therefore, it is conceivable that at a particular instant one or more locations may exist, where the induced velocities form various sources cancel one another giving rise to stationary points.

## 2. Surface Vorticity Method

For the purpose of explanation and to make this presentation more complete, a brief description of this method is given. A more complete account can be found elsewhere, for instance, in Lewis (1991). The complex potential given in equation (1) represents the flow field of free vortices in the presence of bodies. The terms in this equation comprise $M$ surface vorticity elements of unknown strengths $\gamma_m$ and $N$ free vortices of given strengths $\Gamma_j$

$$W = \Phi + i\Psi = \sum_{m=1}^{M} \frac{i\gamma_m ds_m}{2\pi} \log(z - z_m) + \sum_{j=1}^{N} \frac{i\Gamma_j}{2\pi} \log(z - z_j), \tag{1}$$

where $z = x + iy$ represents a point in the flow field, $z_m = x_m + iy_m$ refers to the midpoint in the surface element $s_m$, whose vorticity strength per unit length is $\gamma_m$, and $ds_m$ is the length of this element (fig. 2). The symbol $z_j = x_j + iy_j$ refers to the location of $\Gamma_j$. The circulation $\gamma_m$ or $\Gamma_j$ is defined to be positive when clockwise in accordance with Lewis' convention. The total number of surface vorticity elements is $M$, which may be the sum of several bodies.

The derivative of $W$ gives the velocity components $u$ and $v$ in the $x$- and $y$-direction,

$$u(x,y) = \sum_{m=1}^{M} \frac{\gamma_m ds_m}{2\pi} \frac{y - y_m}{(x - x_m)^2 + (y - y_m)^2} + \sum_{j=1}^{N} \frac{\Gamma_j}{2\pi} \frac{y - y_j}{(x - x_j)^2 + (y - y_j)^2} \tag{2}$$

$$v(x,y) = -\sum_{m=1}^{M} \frac{\gamma_m ds_m}{2\pi} \frac{x - x_m}{(x - x_m)^2 + (y - y_m)^2} - \sum_{j=1}^{N} \frac{\Gamma_j}{2\pi} \frac{x - x_j}{(x - x_j)^2 + (y - y_j)^2}$$

In these two equations as well as in equation (1), variables are given in dimensionless quantities. The characteristic length is $L$, the length of the body, and the characteristic velocity is $\Gamma_o/L$, where $\Gamma_o$ is the representative strength of a free vortex. If we replace $x$ and $y$ in equation (2), which is a field point, by $x_n$ and $y_n$, the coordinates of the surface element $s_n$ (fig. 2), and impose the Dirichlet condition that the internal tangent velocity component is zero, equation (2) become equations (3), which can be used to determine the unknowns $\gamma_m$ in equation (1).

$$\frac{1}{2\pi} \sum_{m=1, m\neq n}^{M} \gamma_m ds_m K_b(s_n, s_m) + \gamma_n \left( \frac{1}{4\pi} \frac{ds_n}{R_n} - \frac{1}{2} \right) = -\frac{1}{2\pi} \sum_{j=1}^{N} \Gamma_j K_v(s_n, z_j), \quad n = 1, \cdots M$$

$$K_b(s_n, s_m) = \frac{(y_n - y_m)\cos\theta_n - (x_n - x_m)\sin\theta_n}{(x_n - x_m)^2 + (y_n - y_m)^2} \tag{3}$$

and

$$K_v(s_n, s_j) = \frac{(y_n - y_j)\cos\theta_n - (x_n - x_j)\sin\theta_n}{(x_n - x_j)^2 + (y_n - y_j)^2}$$

Here $K_b(\ )$ and $K_v(\ )$ are two influence coefficients representing the tangential velocity components at $s_n$ induced by other surface vorticity elements and by free vortices respectively. The symbol $R_n$ is the radius of curvature at $s_n$ and $\theta_n$ the tangential angle (fig. 2). The second term in the first equation accounts for the self-induced velocity of $\gamma_n$ at element $s_n$.

Equations (3) are a linear system of $M$ equations for $M$ unknowns, which can be solved by any standard method. The Gaussian elimination method was used for every example shown here.

With the quantities $\gamma_m$ determined, one can use equations (2) to calculate the convective velocities for vortex $\Gamma_k$ by changing $z$ to $z_k$, where $z_k$ is the position of $\Gamma_k$ at the instant $t$. The evolution of $z_k$ is then given by

$$\frac{dx_k}{dt} = u_k, \quad \frac{dy_k}{dt} = v_k .$$

For a system of $N$ vortices, there are $2N$ such equations, whose solutions give the vortex paths. At each time step one has to update $\gamma_m$, which requires solutions to equations (3). A second-order method is used here for calculating the time development from $t$ to $t + \Delta t$.

$$x_k(t+\Delta t) = x_k(t) + \frac{1}{2}\left[3u_k(t) - u_k(t-\Delta t)\right]\Delta t$$

$$y_k(t+\Delta t) = y_k(t) + \frac{1}{2}\left[3v_k(t) - v_k(t-\Delta t)\right]\Delta t \qquad (4)$$

If the vortices are sufficiently far from the body, it is adequate to calculate vortex paths based on the above procedure. However, if they approach sufficiently close to the surface, accuracy may deteriorate, and precautions should be taken to remedy the situation. Lewis (1991) suggested a few such remedies, which will be followed closely in this note. Some details will be given later.

Before proceeding to solve equations (2) to (4) for a given geometry, it is essential to make a comparison between the exact and numerical predictions. Although it is more convenient to consider a single point vortex in a uniform stream past a circular cylinder, which has exact solutions for any given vortex position, this is not a good comparison, because the vortex motion is partially driven by the free stream. A more stringent test for the present investigation is to consider the trajectories of a vortex pair near an orifice in an infinite body of otherwise still fluid, which was studied by Sheffield (1977). This case is akin to the present investigation, because the presence of free vortices creates the velocity field, and the combined effect of vortices and the orifice determines the vortex paths.

Sheffield considered three cases and had graphical representations for two. His figures contain, however, no numerical information, which makes comparison virtually impossible. For this reason, we recomputed the trajectories in one of his cases by solving numerically the equations given in his paper, which are shown as two dotted lines in figure 3 for two different initial positions, corresponding to those in his figure 2. Although these curves are numerically generated, the governing equations are based on the Schwarz-Christoffel transformation and are exact. By contrast, two solid-line curves in figure 3 obtained by the surface vorticity method are totally numerical. The close agreement in figure 3 suggests that the present method is capable of predicting vortex trajectories in the presence of two bodies (two parts of the orifice). A few particulars are perhaps pertinent. The smallest interval between elements is 0.03L, with L being the half width of the orifice, and the total number of vorticity elements is 144 without recourse to the symmetry property. (Only the lower half is plotted in fig. 3.) A slightly better agreement can still be expected, if surface elements are placed more densely near the sharp corners.

## 3. Geometries of Proposed Device

In order to find locations of stationary points for moving vortices, we begin with the geometry. Two such configurations are shown in figures 4. The device in figure 4(a) is labeled as model A, which is symmetrical both longitudinally and laterally and consists of essentially two forward sections of an NACA-0012 airfoil. The elements at the nose region are picked directly from the coordinates for the NACA-0012 and those in the midsection are obtained by curve fitting to ensure a convex shape. Since the arrangement of surface vorticity elements may affect the appearance of stationary points, coordinates for one such distribution with 17 elements in the forward quadrant are given in table 1. Other distributions with more surface elements have also been used in computations and will be discussed later.

To show that the appearance of stationary points is not an exclusive property of model A, model B is introduced in figure 4(b). This is a simpler geometry than model A, consisting of two parallel surfaces and two semicircular caps. Geometric quantities such as curvatures and tangent lines are known exactly, except at junctions between a circular arc and a straight line.

# 4. Computational Procedure

Models in figure 4 all lie in the upper half plane with a dashed line at $y = 0$ to denote the ground surface. The existence of the ground surface is equivalent to imposing an image system in the lower half plane. Most calculations in this investigation were performed in the upper half plane with the image system included in the influence coefficients in equations (3). See, for example, Lewis for details. A few sample cases were, however, obtained in the entire space to verify the correctness of the half-plane method.

Information needed for computation is as follows. The vortex strength is of unity and the sense is negative (counter-clockwise). It moves from left to right. The time step for a regular run is 0.00375, but it may be reduced to less than 0.000375 if necessary. The computational procedures for two or more vortices are essentially the same as those for a single vortex.

Under the conditions that the vortex is not near the body and the ratio of the local thickness to the length of local element is greater than 0.64 (an empirical quantity by Lewis), accurate numerical solutions can be expected. This ratio is amply satisfied in the present investigation. However, if a vortex moves close to the surface, inaccurate solutions begin to appear. Thus, steps have to be taken to alleviate this problem. Fortunately, stationary points present in the present study are not very near the surface. Nonetheless, we still gave heed to Lewis' precautions. For instance, we made sure that the ratio between the distance from the vortex to the surface and the length of the local element was much greater than 2.0, and the net circulation around the body perimeter due to the externally located vortex was zero in accordance with Kelvin's theorem. If the latter condition was not satisfied, an adjustment was made either according to Lewis' treatment (Chap. 8) or by distributing the unbalanced circulation evenly among all surface elements.

# 5. Results and Discussion

## 5.1. Models A and B with a Single Moving Vortex

Based on the surface element distribution given in table 1, a series of computations for a moving vortex was made, whose results were plotted in figure 5 in the form of a trajectory map. The dotted lines (short dashed lines) represent vortex paths and the long dashed line at the bottom refers to the ground surface. A vortex in the space above the topmost dotted line can slide over the upper body smoothly with some distortion near the surface. Below this line there are two distinct regions, where vortex paths converge to two stationary points. A vortex anywhere in the upper region will converge to the upper stationary point and be trapped there. Likewise, a vortex in the lower region will be trapped by the lower stationary point.

The convergence process to the stationary point is somewhat analogous to the convergence of an infinite series. As a vortex comes close to the stationary station, the translational velocity approaches zero ($10^{-8}$~$10^{-12}$) in the limit and each translational distance is smaller than the one before it.

The fact that a moving vortex in various upstream positions converges spontaneously to the stationary point is somewhat unexpected. One may, therefore, assume that this stationary point is also an equilibrium point. To put it to a test, we displaced a vortex to various arbitrary locations around the stationary point and computed their paths. The finding that these paths all converged to the stationary point in the cases tested is an indication that this assumption is probably correct.

In the computations for figure 5, no values of bound circulation or the Kutta conditions were imposed. As a result, the calculated circulations around two bodies were not zero and were, in fact, a part of the solution. By specifying different values of bound circulations, it is possible to obtain different solutions. These solutions were found to contain no stationary point. Therefore, it seems that for a set of surface elements distributed around an inlet-like device such as model A, there is only one solution that accommodates stationary points.

Lewis' corrective measures stated previously were all adopted here. To satisfy Kelvin's theorem of zero net circulation in a closed loop exterior to a vortex for model A in figure 5, the unbalanced circulation for one case was made to be zero by adjusting the vorticity values on two surface elements nearest to the final position of the stationary vortex. However, in all subsequent computations the unbalanced circulation was distributed equally among surface elements. This latter procedure is deemed to be more reasonable, since we deal with moving vortices especially in the case of spinning. Note that imposing Kelvin's theorem for zero circulation is not the same as making the bound circulation to be zero. (See Lewis, 1991 for details.)

The numerical experiments conducted so far seem to indicate that the appearance of stationary points depends not only on the geometry of the device but also on the arrangement of surface elements. For instance, one can reconfigure the surface element distribution by decreasing or increasing the number of elements or re-arranging elements. Moreover, even though the geometry is symmetric, the element distribution does not have to be. We examined all these cases and found that the locations of stationary points were not fixed. A different distribution would result in a different set of stationary points. Although the new locations are in general only slightly different from those in figure 5, the connecting vortex paths can be substantially dissimilar. In one of these cases with 82 elements per body, there was only one stationary point situated right in front of the lower body somewhat like a stagnation point. For this reason, it is felt that the existence of stationary points is not an exclusive property of the geometry. This raises the question whether stationary points can be easily observed in an experiment by simply installing a device like model A or B.

To demonstrate that geometries other than model A can also accommodate stationary points, a trajectory map for model B with 94 elements per body is plotted in figure 6. This figure is seen to be rather similar to figure 5. As in the previous case, we also re-configured the element distribution and reached the similar conclusion of shifting stationary points. Furthermore, in one case with 126 elements per body, no stationary point was found. This notwithstanding, we believe that there is sufficient evidence to suggest that some sets of vorticity elements distributed around model B are capable of producing stationary points in the flow field.

### 5.2 Vortex in a Uniform Free Stream Velocity

The trajectory maps in figures 5 and 6 were based on the assumption that the body of fluid is motionless at infinity. To remove this restriction and to see the effect of including the free stream velocity, we repeated the necessary computations with the free stream velocity added. Using the free stream velocity $U_\infty$ as the reference velocity, we can add a term in equation (1) to become

$$W = \Phi + i\Psi = \sum_{m=1}^{M} \frac{i\gamma_m ds_m}{2\pi} \log(z - z_m) + \sum_{j=1}^{N} \frac{i\Gamma_j}{2\pi} \log(z - z_j) + z \ , \tag{5}$$

where $z$ in the last term represents the free stream velocity.

Choosing the free stream to be unity, the vortex strength to be $-1.5$, and the remaining conditions to be the same as for figure 6, we carried out the calculations and plotted the results in figure 7. The similarity between figures 6 and 7 is obvious with stationary points approximately at the same locations. The passageway between the space of two bodies in figure 7 is, however, considerably larger. Therefore, the chance for a vortex being trapped is reduced. Note that this is a rather intense vortex. As its strength decreases, the regions, in which vortex paths converge to the stationary points, will contract and eventually disappear altogether.

### 5.3 Model A with Two or Three Moving Vortices

In the above we presented trajectory maps for two different models, which have the capability of trapping a single moving vortex. It would be of interest to see whether this capability remains effective as two or more vortices are introduced. The answer is affirmative as indicated by the sample cases in figures 8 to 10. No trajectory maps are, however, given, partly because of the difficulty of laying out a map with multiple vortices. The surface element distribution adopted for these computations was somewhat different from that used for figure 5. The present

distribution had 90 elements per body instead of 66 elements per body. The purpose is simply to show that both distributions accommodate stationary points.

The vortices shown in these figures are of equal strength and of the same sense. Therefore, they rotate about the centroid at a constant speed and move nearly parallel to the ground surface from left to right initially, since the presence of the device is only scantly felt. This is the reason that the trajectories far from the device are equally coiled. For a group of two or more vortices placed uniformly around the circumference of a circle of radius a and in a free space of still fluid, they will undergo circular motions at a constant angular velocity $\Omega$ given by the equation (Saffman, 1992, Chap. 7)

$$\Omega = (n-1)\frac{\Gamma}{4\pi a^2}, \tag{6}$$

where $n$ is the number of vortices and $\Gamma$ is the strength.

We first study the fate of a pair of spinning vortices moving from left to right. Four sets of these trajectories were depicted in figures 8 and 9, two in each figure. As in earlier cases for a single vortex, each set was computed separately. The purpose of figure 8 is to show that the stationary points for a pair lie approximately at the same places as in figure 5, and the purpose of figure 9 is to demonstrate that two pairs of vortices can converge to the same stationary point much like a single vortex. In figure 8 the vortex strength of these two pairs is the same but the separation distances are different. Thus, the upper pair spins slower than the lower pair. We regard the two dark disks to be the stationary stations, because at these stations the forward motion of the centroid ceases, but the vortices continue to rotate. If the centroid wobbles a little and the spinning radius changes a little, the vortex paths after a long period of time cover the entire area, which then becomes black. (The vortex strength and the time step chosen for these two cases were unity and 0.001875 respectively.)

We now consider the case of three like-signed vortices of the equal strength with the angular velocity given by equation (6). This is a triad of spinning vortices much like a pair of spinning vortices. The uniform coiling of upstream vortex trajectories in figure 10 attests to this assertion. Two sets of initial conditions for these triads were selected to lay claim that they will be captured like a single vortex. This is shown in figure 10. Finally, it is noted parenthetically that similar trajectory patterns for spinning vortices, though not shown, have been obtained for model B.

## 6. Concluding Remarks

It is seen in the above that stationary points can occur in two types of inlet-like devices. The geometry of the device appears to play a more important part in determining the existence of stationary points, but the role of the element distribution pattern cannot be neglected. It is not, however, clear at this stage the relationship between these two or how to separate one from the other. Further study is needed.

Since both models can accommodate stationary points, it is reasonable to assume that there are other configurations that have the similar property.

Although the space between two bodies and the height of the lower body from the ground surface were fixed at 70 and 50 percent body length in the present study, different values of these lengths have been examined. As far as the space between two bodies is concerned, it can be as large as 1.5 times body length and still accommodate stationary points.

The trajectory maps in figures 5 to 7 point to the fact that there are two zones, one for each body. Thus, there is a likelihood that three or more bodies can be stacked together to produce three or more zones with one stationary point for each body.

The preceding evidence suggests that two or three spinning vortices can have similar characteristics of a single vortex. Therefore, it is possible that some of the present findings are valid for a vortex with a finite core, since a group of spinning vortices bears some resemblance to a vortex with a finite core.

# References

Aref, H., Kadtke, J.B., Zawadzki, I., Campbell, L.J. and Eckhardt, B., 1988: "Point vortex dynamics: recent results and open problems," Fluid Dynamics Res. **3**, pp. 63–74.

Lewis, R.I., 1981: "Surface vorticity modelling of separated flows from two-dimensional bluff bodies of arbitrary shape," J. Mech. Engng Sci., **23**, pp. 1–12.

Lewis, R.I., 1991: Vortex Element Methods for Fluid Dynamic Analysis of Engineering Systems, Cambridge University Press, New York, N.Y.

Martensen, E., 1959: "Berechnug der druckverteilung an pitterprofilen in ebener potentialstromung mit einer Fredholmschen integralgleichungen," Arch. Rat. Mech. Anal., **3**, pp. 235–270.

Saffman, P.G., 1992: Vortex Dynamics. Cambridge University Press, New York, N.Y.

Sheffield, J.S., 1977: "Trajectories of an ideal vortex pair near an orifice," Phy. Fluids, **20**, pp. 543–545.

TABLE 1.—COORDINATES FOR MODEL A ON THE FORWARD QUADRANT

| x | y |
|---|---|
| 0.0020000 | 0.0078146 |
| .0050000 | .0122131 |
| .0080000 | .0153151 |
| .0120000 | .0185770 |
| .0180000 | .0224718 |
| .0360000 | .0308125 |
| .0700000 | .0408627 |
| .1000000 | .0468276 |
| .1300000 | .0511933 |
| .1600000 | .0544181 |
| .2050000 | .0576546 |
| .2500 | .0598 |
| .3000 | .0619 |
| .3500 | .06327 |
| .4000 | .0641 |
| .4500 | .06467 |
| .5000 | .06483 |

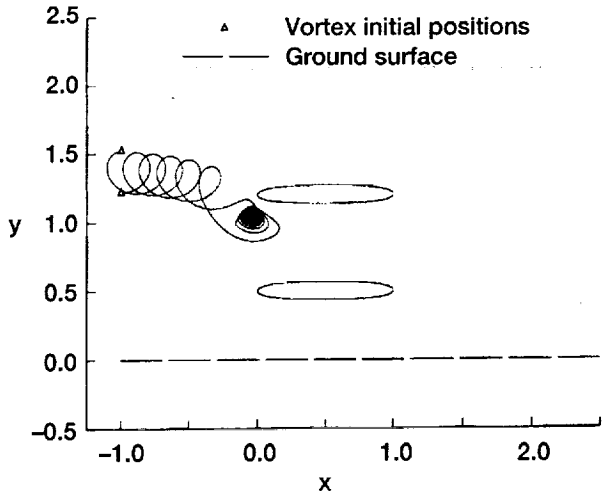


Figure 1.—A pair of spinning vortices trapped by an inlet-like device as it moves from left to right.

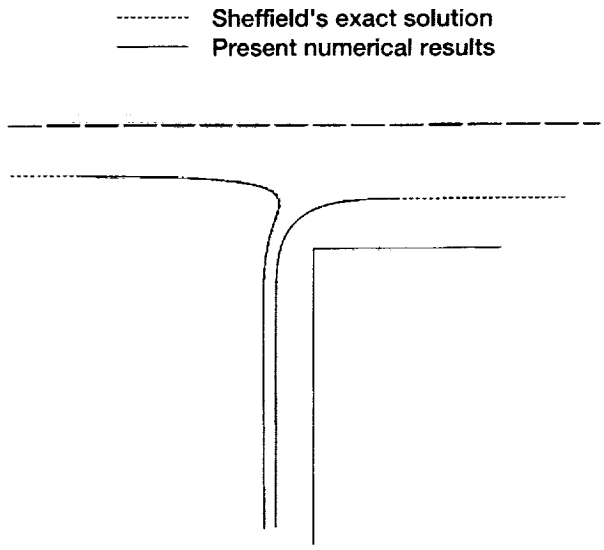


Figure 3.—Lower-half trajectories of an ideal vortex pair approaching an orifice.

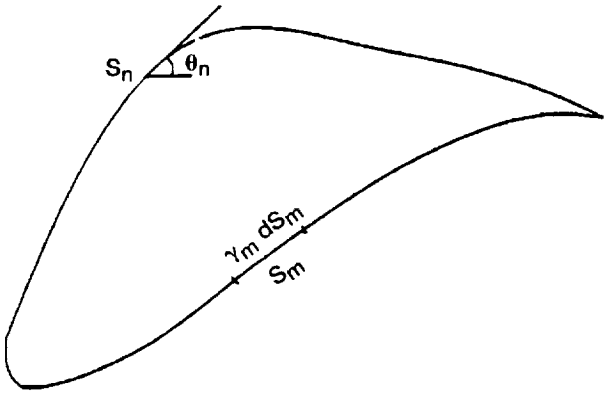


Figure 2.—Surface vorticity elements on a two-dimensional body.

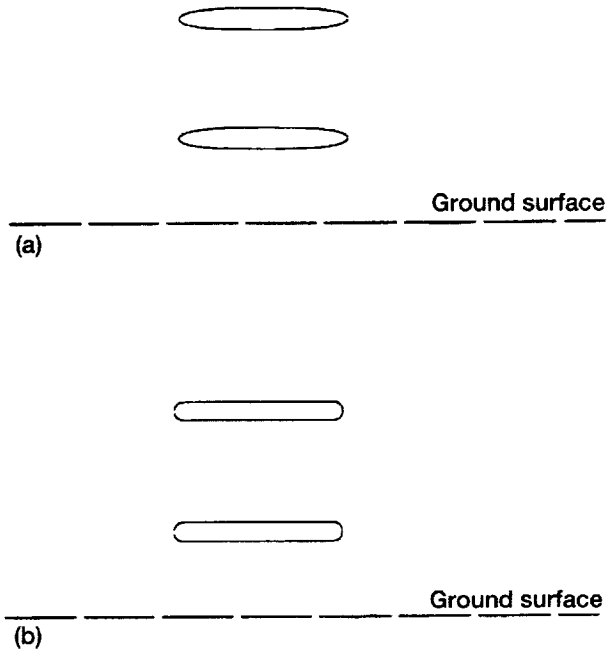


Figure 4.—Geometry of an inlet-like device. (a) Model A. (b) Model B.

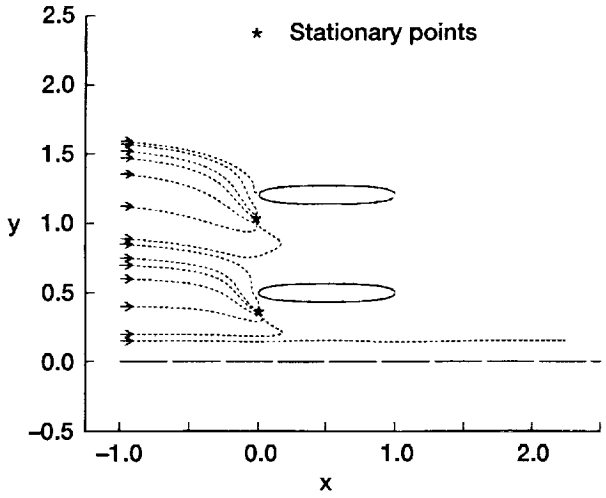


Figure 5.—Vortex trajectory map with model A for a single vortex moving from left to right.

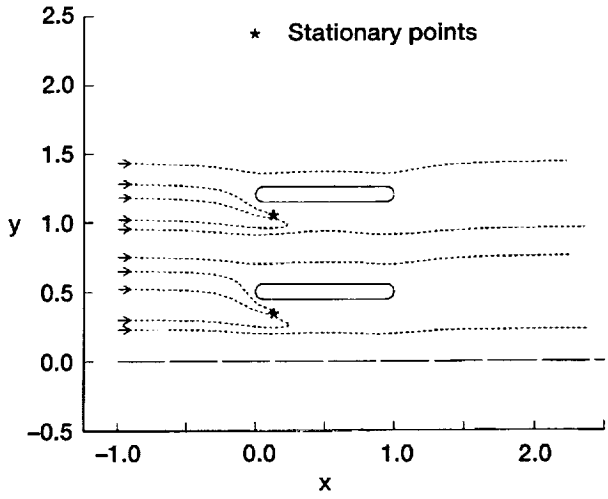


Figure 7.—Vortex trajectory map with model B for a single vortex moving from left to right in a uniform stream flowing from left to right. Vortex strength = −1.5.

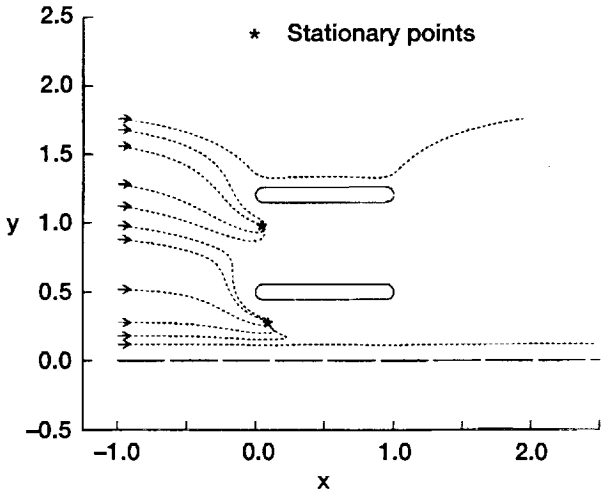


Figure 6.—Vortex trajectory map with model B for a single vortex moving from left to right.

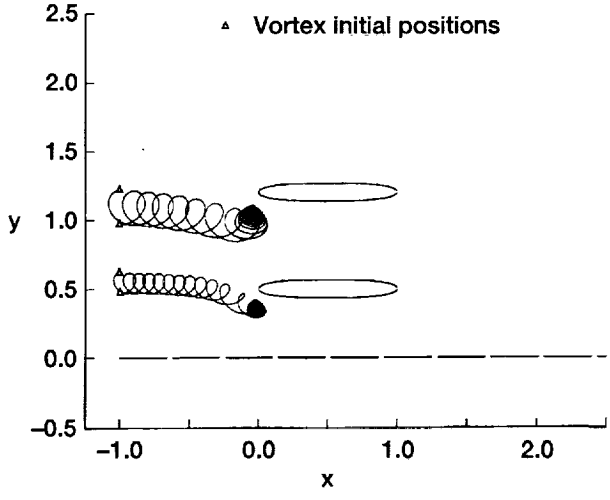


Figure 8.—A pair of spinning vortices trapped by model A as it moves from left to right from two different initial positions.

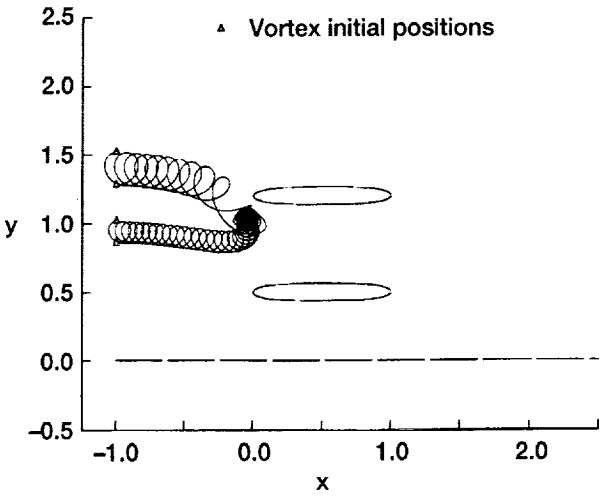


Figure 9.—A pair of spinning vortices trapped by model A as it moves from left to right from two different initial positions.

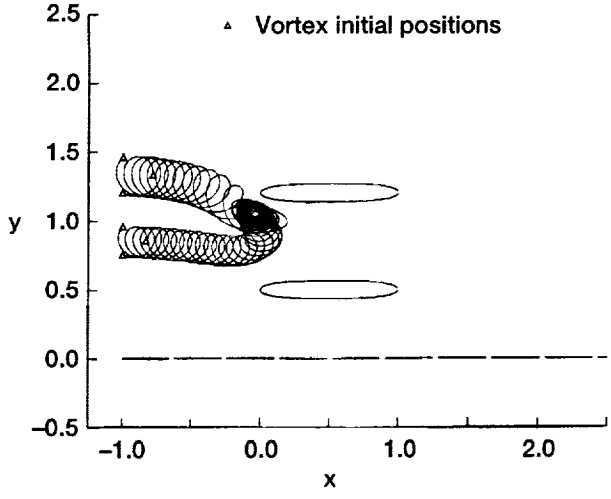


Figure 10.—A triad of spinning vortices trapped by model A as it moves from left to right from two different initial positions.

# REPORT DOCUMENTATION PAGE

*Form Approved*
*OMB No. 0704-0188*



| 1. AGENCY USE ONLY (*Leave blank*) | 2. REPORT DATE | 3. REPORT TYPE AND DATES COVERED |
|---|---|---|
| | July 2000 | Technical Memorandum |

**4. TITLE AND SUBTITLE**

A Note on Trapping Moving Vortices

**5. FUNDING NUMBERS**

WU-522-31-23-00

**6. AUTHOR(S)**

Hsiao C. Kao

**7. PERFORMING ORGANIZATION NAME(S) AND ADDRESS(ES)**

National Aeronautics and Space Administration
John H. Glenn Research Center at Lewis Field
Cleveland, Ohio 44135-3191

**8. PERFORMING ORGANIZATION REPORT NUMBER**

E-11720

**9. SPONSORING/MONITORING AGENCY NAME(S) AND ADDRESS(ES)**

National Aeronautics and Space Administration
Washington, DC 20546-0001

**10. SPONSORING/MONITORING AGENCY REPORT NUMBER**

NASA TM—2000-209270

**11. SUPPLEMENTARY NOTES**

Responsible person, Hsiao C. Kao, organization code 5860, (216) 433-5866.

**12a. DISTRIBUTION/AVAILABILITY STATEMENT**

Unclassified - Unlimited
Subject Category: 02 Distribution: Nonstandard

This publication is available from the NASA Center for AeroSpace Information, (301) 621-0390.

**12b. DISTRIBUTION CODE**

**13. ABSTRACT** ***(Maximum 200 words)***

The topic of stationary configurations of point vortices, also known as vortex equilibrium, has received considerable attention in recent years. By observing numerical results, it is found that a "counterpart" of this system also exists, in which moving vortices may be "trapped" by an inlet-like device to form a stationary pattern with no translational motion. After an intuitive explanation for the process, vortex trajectory maps based on numerical results are presented. These maps exhibit two stationary points under the present conditions, which are the focal points of vortex trajectories. A vortex upstream of these points, if within a certain offset range, will move towards these points spontaneously and be captured there. This proposed device is also capable of trapping spinning vortex pairs and triads. It is possible to impose a uniform stream at infinity, as long as the flow field is still dominated by the moving vortices.

**14. SUBJECT TERMS**

Vortex; Vortex-body interaction; Spinning pairs or triads; Ground surface

**15. NUMBER OF PAGES**
16

**16. PRICE CODE**
A03

| 17. SECURITY CLASSIFICATION OF REPORT | 18. SECURITY CLASSIFICATION OF THIS PAGE | 19. SECURITY CLASSIFICATION OF ABSTRACT | 20. LIMITATION OF ABSTRACT |
|---|---|---|---|
| Unclassified | Unclassified | Unclassified | |